

# Overexpression, Amplification, and Androgen Regulation of TPD52 in Prostate Cancer

Mark A. Rubin,<sup>1,2</sup> Sooryanarayana Varambally,<sup>3</sup> Rameen Beroukhi,<sup>2,7</sup> Scott A. Tomlins,<sup>3</sup> Daniel R. Rhodes,<sup>3</sup> Pamela L. Paris,<sup>8</sup> Matthias D. Hofer,<sup>1,2</sup> Martina Storz-Schweizer,<sup>1,2</sup> Rainer Kuefer,<sup>9</sup> Jonathan A. Fletcher,<sup>1,2</sup> Bae-Li Hsi,<sup>1</sup> Jennifer A. Byrne,<sup>10</sup> Kenneth J. Pienta,<sup>4,5,6</sup> Colin Collins,<sup>8</sup> William R. Sellers,<sup>2,7</sup> and Arul M. Chinnaiyan<sup>3,4,6</sup>

<sup>1</sup>Department of Pathology, Brigham and Women's Hospital, Boston, Massachusetts; <sup>2</sup>Harvard Medical School, Boston, Massachusetts; <sup>3</sup>Departments of <sup>3</sup>Pathology, <sup>4</sup>Urology, and <sup>5</sup>Internal Medicine and <sup>6</sup>Comprehensive Cancer Center, University of Michigan Medical School, Ann Arbor, Michigan; <sup>7</sup>Dana-Farber Cancer Institute, Boston, Massachusetts; <sup>8</sup>Comprehensive Cancer Center, University of California at San Francisco, San Francisco, California; <sup>9</sup>Department of Urology, University Hospital of Ulm, Ulm, Germany; and <sup>10</sup>Molecular Oncology Laboratory, Oncology Research Unit, The Children's Hospital at Westmead, New South Wales, Australia

## ABSTRACT

Gains in the long arm of chromosome 8 (8q) are believed to be associated with poor outcome and the development of hormone-refractory prostate cancer. Based on a meta-analysis of gene expression microarray data from multiple prostate cancer studies (D. R. Rhodes *et al.*, *Cancer Res* 2002;62:4427–33), a candidate oncogene, *Tumor Protein D52 (TPD52)*, was identified in the 8q21 amplicon. TPD52 is a coiled-coil motif-bearing protein, potentially involved in vesicle trafficking. Both mRNA and protein levels of TPD52 were highly elevated in prostate cancer tissues. Array comparative genomic hybridization and amplification analysis using single nucleotide polymorphism arrays demonstrated increased DNA copy number in the region encompassing TPD52. Fluorescence *in situ* hybridization on tissue microarrays confirmed TPD52 amplification in prostate cancer epithelia. Furthermore, our studies suggest that TPD52 protein levels may be regulated by androgens, consistent with the presence of androgen response elements in the upstream promoter of TPD52. In summary, these findings suggest that dysregulation of TPD52 by genomic amplification and androgen induction may play a role in prostate cancer progression.

## INTRODUCTION

Genetic alterations are believed to accumulate in the course of neoplastic progression. In prostate cancer, progression has been associated with early and late molecular events. Loss of the short arm of chromosome 8 (8p) is considered an early event and is seen in prostatic intraepithelial neoplasia and nearly all prostate cancers (1–5). Later events such as gains of the long arm of chromosome 8 (8q) have been implicated in the progression to more aggressive prostate cancer (1, 2, 6–9). The critical sites of 8q gain include 8q21 (10–12) and 8q23–24 (13–17). *Elongin C* was proposed as a putative prostate cancer oncogene amplified at 8q21(12). The *c-myc* oncogene located at 8q24 has also been found to be variably amplified in prostate cancer (7, 15, 16, 18, 19).

Here we present data supporting the role of TPD52 as a candidate oncogene. TPD52, located on 8q21(20), has previously been demonstrated to be amplified and overexpressed in breast cancer (21, 22). We demonstrate through cDNA expression array analysis and immunohistochemistry that TPD52 is overexpressed in prostate cancer.

Received 12/11/03; revised 3/5/04; accepted 3/17/04.

**Grant support:** Specialized Program of Research Excellence for Prostate Cancer National Cancer Institute Grants P50CA90381 (M. A. Rubin) and P50CA69568 (K. J. Pienta, M. A. Rubin, and A. M. Chinnaiyan), National Cancer Institute Grants CA 97063 (A. M. Chinnaiyan and M. A. Rubin) Department of Defense grant DAMD17-03-2-0033 (M.A. Rubin and A.M. Chinnaiyan) and R01AG21404 (M. A. Rubin), and American Cancer Society Grant RSG-02-179-MGO (A. M. Chinnaiyan Department of Defense (M.A. Rubin and A.M. Chinnaiyan) and M. A. Rubin).

The costs of publication of this article were defrayed in part by the payment of page charges. This article must therefore be hereby marked *advertisement* in accordance with 18 U.S.C. Section 1734 solely to indicate this fact.

**Note:** M. A. Rubin and S. Varambally contributed equally to this work.

**Requests for reprints:** Mark A. Rubin, Department of Pathology (Amory 3-195), Brigham and Women's Hospital/Harvard Medical School, 75 Francis Street, Boston, MA 02115. Phone: (617) 525-6747; Fax: (617) 264-5169; E-mail: marubin@partners.org.

Array comparative genomic hybridization (aCGH), amplification analysis using single nucleotide polymorphism (SNP) chips, and fluorescence *in situ* hybridization (FISH) all implicate amplification of the chromosomal region containing TPD52. A survey of gene expression studies provides evidence that TPD52 is overexpressed in several other common human malignancies.

## MATERIALS AND METHODS

**Patient Population and Tissue Collection.** Prostate tissue samples were taken from the radical prostatectomy series and the rapid autopsy program at the University of Michigan Prostate Cancer Specialized Program of Research Excellence Tissue Core with institutional review board approval. Clinically localized prostate cancer samples used for this study were taken from a cohort of men who underwent radical retropubic prostatectomy as a monotherapy (*i.e.*, no hormonal or radiation therapy) for clinically localized prostate cancer between January 1995 and December 2001. Tumors were staged using the tumor-node-metastasis (TNM) system (23) and graded according to the system originally described by Gleason (24, 25). The snap-frozen samples used for immunoblot, aCGH, and SNP analysis were all evaluated histologically by the study pathologist (M. A. R.). All samples were trimmed to ensure that >95% of the sample used represented the desired lesion. Hormone-refractory metastatic prostate cancer samples from 15 autopsy cases performed from 1997 to 2000 were also collected from the rapid ("warm") autopsy program (26). The patients' ages ranged from 40 to 84 years, with a median age of 67.5 years. Hormone-naïve metastatic prostate cancers were collected at the University of Ulm Hospital as part of an ongoing institutional review board-approved research program to study the molecular signature of metastatic prostate cancer.

**Quantitative Real-Time PCR.** Quantitative real-time PCR for TPD52 expression was performed using SYBR Green essentially as described previously (27). Briefly, total RNA isolated from 11 benign prostate samples, 33 clinically localized prostate cancer samples, and 15 metastatic prostate cancer samples was reverse transcribed into first-strand cDNA. The quantity of cDNA in each sample was calculated by interpolating its  $C_t$  value versus a standard curve of  $C_t$  values obtained from serially diluted cDNA from commercially available pooled normal prostate samples (Clontech) and one of the prostate cancer samples. The calculated quantity of TPD52 for each sample was then divided by the quantity of the housekeeping gene *glyceraldehyde-3 phosphate dehydrogenase (GAPDH)*, *hydroxymethylbilane synthase (HMBS)*, or the average of GAPDH and HMBS corresponding to each sample to give a relative expression of TPD52 for each sample. HMBS, a pseudogene-free gene, has been shown in previous studies, including studies of neoplastic versus normal tissue (27–30), to be an accurate housekeeping gene in a variety of tissues. Through validation with over 40 genes identified as being differentially expressed in prostate cancer, we found that the addition of HMBS as a second internal control improves our correlation to cDNA microarray data, consistent with other reports (31). No reverse transcription controls were included when the 3'-untranslated region primers were used. Primer sequences (5' to 3') are as follows: TPD52\_cds-sense, GCTGCTTTTTCGTCTGTTGGCT3; TPD52\_cds-antisense, TCAAATGATTTAAAAGTTGGGGAGTT; TPD52\_3'UTR-sense, CATCCTGGCCTGCTACTAATCTT; and TPD52\_3'UTR-antisense, CACT-TGCCACCCCATTTCTATC. GAPD and HMBS primers were as described previously (2).

**Cell Culture and Androgen Treatment.** LNCaP cells (American Type Culture Collection, Manassas, VA) were grown in RPMI 1640 without phenol red (Sigma, St. Louis, MO) supplemented with 10% fetal bovine serum (BioWhittaker), 2 mM L-glutamine, 50 units/ml penicillin, and 50  $\mu$ g/ml streptomycin. Cells were maintained in a 5% CO<sub>2</sub>, 95% air-humidified atmosphere at 37°C and cultured in phenol red-free medium with 5% stripped fetal bovine serum (BioWhittaker) 48 h before experiments. The cells were plated on 100-mm dishes with 50% density. Forty-eight h later, the cells were treated with either vehicle control or 1 nM synthetic androgen R1881 (New England Nuclear).

**Immunoblot Analyses.** Tissues were homogenized in NP40 lysis buffer containing 50 mM Tris-HCl (pH 7.4), 1% NP40 (Sigma), and complete proteinase inhibitor mixture (Roche). Fifteen  $\mu$ g of protein extracts were mixed with SDS sample buffer and electrophoresed onto a 10% SDS-polyacrylamide gel under reducing conditions. The separated proteins were transferred onto nitrocellulose membranes (Amersham Pharmacia Biotech, Piscataway, NJ). The membrane was incubated for 1 h in blocking buffer [Tris-buffered saline with 0.1% Tween (TBS-T) and 5% nonfat dry milk]. The affinity-purified TPD52 rabbit polyclonal antibody (22) was applied at a 1:1,000 dilution in blocking buffer overnight at 4°C. After washing three times with TBS-T buffer, the membrane was incubated with horseradish peroxidase-linked donkey antirabbit IgG antibody (Amersham Pharmacia Biotech) at a 1:5,000 dilution for 1 h at room temperature. The signals were visualized with the enhanced chemiluminescence detection system (Amersham Pharmacia Biotech) and autoradiography. To monitor equal loading, the TPD52 antibody-probed membrane was stripped with Western Re-Probe buffer (Geno-tech, St. Louis, MO), blocked in TBS-T with 5% nonfat dry milk, and incubated with rabbit anti-GAPDH antibody (1:25,000 dilution; Abcam, Cambridge, MA) and anti-heterochromatin protein  $\beta$  (HP1 $\beta$ ; 1:1,000 dilution; Upstate, Charlottesville, VA) for 2 h. In prostate cancer, many epithelial cell proteins show differential expression. Changes in keratin expression during the development of benign prostatic hyperplasia and prostate cancer have been reported (32, 33). Hence we did not use keratins as controls.

**Immunohistochemistry.** Sections of 4- $\mu$ m-thick, paraffin-embedded tissue microarrays (TMAs) were dewaxed and rehydrated using xylene and ethanol, respectively. After immersion in 10 mM citrate buffer (pH 6.0), the slides underwent microwave pretreatment for 10 min for optimal antigen retrieval. The affinity-purified TPD52 rabbit polyclonal antibody (22) was incubated overnight in a 1:20 dilution at 4°C. The secondary antibody was labeled with biotin and applied for 30 min. Streptavidin-LSA amplification method (DAKO K0679) was carried out for 30 min followed by peroxidase/diaminobenzidine substrate/chromagen. The slides were counterstained with hematoxylin. Protein expression was scored as negative (score = 1), weak (score = 2), moderate (score = 3), or strong (score = 4) using a system that has been validated previously (34–39).

**Tissue Microarray Construction, Digital Image Capture, and Analysis.** As described previously, high-density (TMAs) composed of samples from a wide range of prostate tissues were assembled using a manual tissue arrayer [Beecher Instruments, Silver Spring, MD (34, 40–42)]. Three to four 0.6-mm tissue cores were taken from each targeted lesion (*i.e.*, benign, prostate cancer, or metastatic prostate cancer) and placed into a recipient block. Digital images were acquired from the 4- $\mu$ m-thick H&E-stained sections as well as all immunostained TMA slides using the BLISS Imaging System (Bacus Laboratory, Lombard, IL). Protein expression was evaluated in a blinded manner using an internet-based TMA presentation tool, TMA Profiler.<sup>11</sup> The tissue sample diagnosis was confirmed, and immunostaining was scored by the study pathologist for protein expression intensity as described above.

**Array Comparative Genomic Hybridization.** The aCGH protocol that was followed has been reported recently (43–45). In brief, the human version 2.0 bacterial artificial chromosome (BAC) arrays were provided by the University of California at San Francisco Array Core Facility. In aCGH, microarrayed BAC DNA targets are cohybridized with differentially fluorophore-labeled DNAs from normal reference and tumor test genomes. Primary Tumor DNA was prepared from microdissected archival material (43). Genomic gain was defined a log<sub>2</sub> ratio greater than or equal to the tumor background threshold (43). Gene copy number along the genome is proportional to the ratio

of fluorescent intensities. Each array consists of 2460 BACs spotted in triplicate on chromium slides that provides a resolution of approximately 1.4 Mb. All clones have been mapped on the University of California at Southern California genome assembly<sup>12</sup> and can be computationally linked to the underlying and annotated genome sequence. Seven consecutive clones were identified at 8q21 that were used to help determine the amplicon size.

**Copy Number of TPD52 Was Determined by SNP Arrays.** Copy numbers were determined by analysis of SNP arrays (46). The protocol used to determine copy number from SNP arrays is reported separately (47). Briefly, DNA was digested with *Xba*I, ligated to a single primer, and subjected to single primer extracted from a 2-mm core of each metastasis using a Qiagen Mini-Prep kit (Valencia, CA). It was then subjected to PCR amplification under conditions favoring the generation of 200-bp amplicons. These amplicons were then fragmented, fluorophore labeled, and hybridized to an Affymetrix SNP array containing over 400,000 probes interrogating over 116,500 SNP loci (48). Using the informatics platform dChip (49), signal intensities at each probe locus were analyzed compared with a composite reference, representing germ-line DNA from 19 individuals, to determine copy number at each SNP locus using methods described previously (47). The region displayed represents data obtained from over 60 SNPs at 8q21 with 3 SNPs within the region spanned by *TPD52*.

**Quantitative Real-Time PCR to Validate Copy Number.** Quantitative real-time PCR was performed on a PRISM 7700 sequence detector (Applied Biosystems) and Opticon Chromo 4 (MJ Research) using a QuantiTect SYBR Green kit (Qiagen). We have quantified each tumor DNA by comparing the target locus to the reference Line-1, a repetitive element for which copy numbers per haploid genome are similar among all human normal and neoplastic cells (50). Quantification is based on standard curves from a serial dilution of human normal genomic DNA. The relative target copy number level was also normalized to normal human genomic DNA as a calibrator. Copy number change of target gene relative to the Line-1 and the calibrator was determined by using the formula  $(T_{\text{target}}/T_{\text{Line-1}})/(C_{\text{target}}/C_{\text{Line-1}})$ , where  $T_{\text{target}}$  and  $T_{\text{Line-1}}$  are quantity from tumor DNA by using target and Line-1, and  $C_{\text{target}}$  and  $C_{\text{Line-1}}$  are quantity from calibrator by using target and Line-1. PCRs for each primer set were performed in at least triplicate, and means were reported. Conditions for quantitative PCR reaction were as follows: one cycle of 50°C for 15 min; one cycle of 94°C for 2 min; and 40 cycles of 94°C for 20 s, 56°C for 20 s, and 70°C for 20 s. At the end of the PCR reaction, samples were subjected to a melting analysis to confirm specificity of the amplicon. Primers were designed by using Primer 3<sup>13</sup> to span a 100–150-bp nonrepetitive region and synthesized by Invitrogen. Each primer set was subsequently compared with the human genome using the BLAST algorithm to determine its uniqueness. All primer sets were further confirmed to generate a single desired size amplicon evaluated by gel electrophoresis. For homozygous deletion, the presence or absence of PCR products was also evaluated by agarose gel electrophoresis. Primer sequences for each target used in this study are published as the supporting information. Primer sequences (designed to include both intronic and exonic elements in the amplicon, to avoid amplification of mRNA) were as follows: LINE-1, AAAGCCGCTCAACTACATGG (forward) and TGCTTTGAATGCGTCCCAGAG (reverse); exon 2, ATGGTTAAATCCCCAACCA (forward) and TCTTCCGAGAGGGTCTCTGT (reverse); exon 4, GAGCTGACCCTTCTTTTGTCT (forward) and GACTGAGCCAACAGACGAAA (reverse); and exon 6, TGGTGGTGATTTTGGAGAAG (forward) and GCAGTGGGTAGCAGAACAAA (reverse).

**Fluorescent *In Situ* Hybridization for *TPD 52/Elongin c*.** TMA sections were pretreated with a 50 mM Tris and 100 mM EDTA solution at 199°F for 15 min and digested with Digest All 3 (Zymed, South San Francisco, CA) for 3 min. The TMAs and BAC FISH probes were then codenatured at 94°C for 3 min and hybridized overnight at 37°C. The BAC FISH probes were digoxigenin-labeled BAC RP11–367E12 probe for the *Elongin c* gene (*TCEB1*) and the biotin-labeled BAC probes RP11–941H19 and RP11–92K15 for the *TPD52* gene. Posthybridization washing was with 0.5 $\times$  SSC for 5 min, and the fluorescence detection was carried out using anti-digoxigenin-FITC and streptavidin-Alexa-594 conjugates (Molecular Probes, Eugene, OR). Slides were then counterstained and mounted in 4',6-diamidino-2-phenylindole-Vectashield (Vector Laboratories, Burlingame, CA). FISH signals were ana-

<sup>11</sup> <http://rubinlab.tch.harvard.edu>.

<sup>12</sup> <http://genome.ucsc.edu/index.html>.

<sup>13</sup> [http://www-genome.wi.mit.edu/cgi-bin/primer/primer3\\_www.cgi](http://www-genome.wi.mit.edu/cgi-bin/primer/primer3_www.cgi).

lyzed using the Oncor Imaging System, and images were captured using a charge-coupled device camera (Photometrics, Tucson, AZ).

**Statistical Analysis.** Pertinent clinical information [*i.e.*, clinical stage, pre-treatment prostate-specific antigen (PSA), tumor stage, surgical margin status, and Gleason score] was prospectively collected. Clinical postprostatectomy follow-up was also ascertained and stored prospectively, including an annual patient assessment by clinic visit, phone, or mail contact to ascertain overall, cancer-specific, and PSA recurrence-free survival. A PSA level of >0.2 ng/ml was considered biochemical evidence of micrometastatic recurrence or progression. TPD52 protein expression was evaluated as a mean score based on all TMA cores from a single patient. Expression was graphically represented using error bars with 95% confidence intervals. Differences between tissue types (*e.g.*, benign *versus* localized prostate cancer) were evaluated using ANOVA with a *post hoc* Scheffe analysis to take multiple tissue types into account. The association of clinical parameters, pathology results, and TPD52 expression with recurrence-free survival was first evaluated by bivariate (univariate) analysis. The relationship between preoperative variables and recurrence-free survival was then examined using Cox proportional-hazard regression models. All decisions were made using a 0.05 significance level, and all analyses were run using the SPSS software (SPSS Systems, Chicago, IL).

**RESULTS**

**Meta-Analysis of DNA Microarray Studies Demonstrates Overexpression of TPD52 Transcript in Prostate Cancer.** Meta-analysis of prostate cancer profiling studies (51) has identified several markers of prostate cancer including *hepsin*, *AMACR*, and *fatty acid synthase* (34, 52–56). *TPD52* was a gene identified by this meta-analysis (Fig. 1A; Ref. 51) and also found in a region often amplified in prostate cancer, chromosome 8q21 (7, 20). Based on the four prostate expression array data sets, overexpression of *TPD52* was observed in prostate cancer samples (*n* = 63) when compared with histologically benign prostate tissue (*n* = 32) with a false discovery rate (Fig. 1A, *FDR*) of 0.05. Overexpression of the *TPD52* transcript in prostate cancer was validated using quantitative reverse transcription-PCR (Fig. 1B). Box plot representations of the quantitative reverse transcription-PCR data demonstrate a significant increase in the mRNA level of *TPD52* in clinically localized prostate cancer (*P* = 1e-5; Fig. 1C).

**Overexpression of TPD52 Protein in Prostate Cancer.** To determine whether *TPD52* overexpression at the transcript level corresponded with overexpression at the protein level, prostate tissue

extracts were prepared from benign prostate tissue, prostate cancer, and metastatic prostate tumors, and immunoblot analysis was performed using an affinity-purified antibody specific for *TPD52* (22, 57). Consistent with the *TPD52* mRNA results, *TPD52* protein levels were elevated in clinically localized prostate cancer and metastatic prostate cancer compared with benign prostate tissue samples. No changes in expression were appreciated with the two control genes (*HPIβ* and *GAPDH*) between the different tissue types (Fig. 2A).

**Immunohistochemistry Using High-Density Tissue Microarrays Confirmed TPD52 Protein Overexpression in Prostate Cancer.** To validate that overexpression of the *TPD52* transcript was associated with overexpression at the protein level, we performed immunohistochemistry using the affinity-purified polyclonal antibody against *TPD52*. Using high-density prostate cancer TMAs, we were able to characterize *TPD52* protein expression in a wide range of prostate samples. *TPD52* protein expression was cytoplasmic, consistent with a previous report in breast cancer (22). Weak to moderate *TPD52* expression was seen in benign prostate tissue (Fig. 2B, 1 and 2). Strong protein expression was consistently seen in clinically localized prostate cancer samples (Fig. 2B, 3 and 4) and metastatic prostate cancer (Fig. 2B, 5). *TPD52* expression was confined to the cytoplasm and was not observed in the nucleus (Fig. 2B, 6). Protein expression was strongest in clinically localized and metastatic prostate cancer. The mean *TPD52* protein expression levels are presented in Table 1 and Fig. 2C. There was no significant difference seen between clinically localized prostate cancer and hormone-refractory prostate cancer. In a subset of 54 cases of clinically localized prostate cancer (*i.e.*, clinical stage T<sub>1a-c</sub> or T<sub>2</sub>), we looked for associations with PSA failure after radical prostatectomy for clinically localized prostate cancer. In this cohort, 37% (7 of 19) failures were seen in *TPD52* high expressors in contrast to 20% (7 of 35) failures in moderate expressors. These differences demonstrated a trend toward higher PSA failure rates in men with high-*TPD52*-expressing tumors (log rank *P* = 0.12). No significant associations were observed between *TPD52* protein expression and Gleason score, tumor stage, or surgical margin status.

**Androgen Regulation of TPD52 Protein.** Sequence analysis demonstrated the presence of androgen-responsive elements in the putative promoter region of *TPD52* (Ref. 58; Fig. 2D). The hormone-responsive prostate cancer cell line LNCaP was treated with the

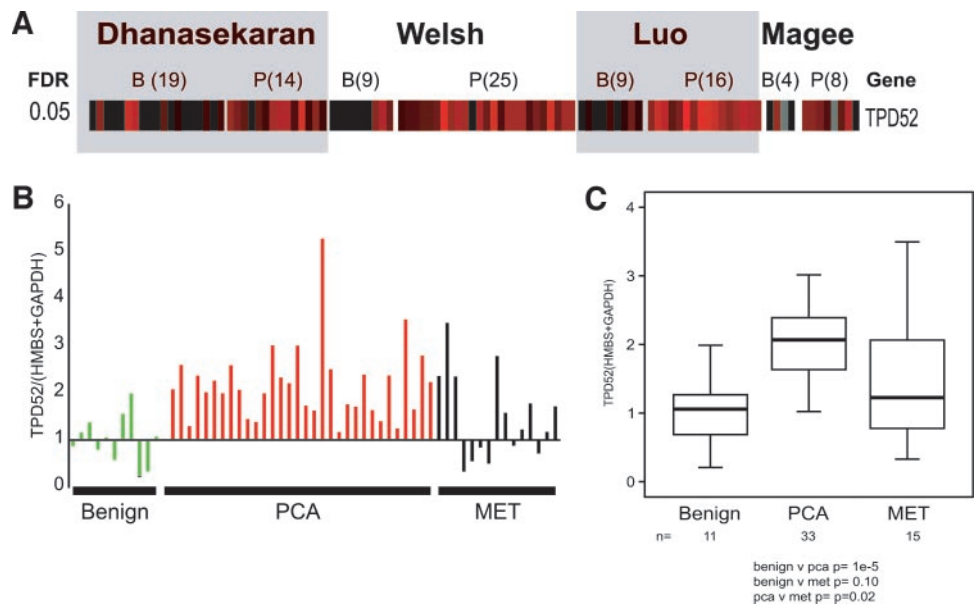


Fig. 1. A–C, overexpression of *TPD52* transcript in prostate cancer. A, Eisen matrix representation of *TPD52*, which is differentially expressed between clinically localized prostate cancer (P) and benign prostate tissue (B), across four independent microarray studies (51). Quantitative reverse transcription-PCR of *TPD52* transcripts shown from benign prostate tissue (*n* = 11), localized prostate cancer (*n* = 33), and metastatic prostate cancer (*n* = 15). B and C, the ratio of *TPD52* expression was normalized against an average of *HMBS* and *GAPDH* expression (B), and this is graphically presented as box plots with 95% confidence intervals (C).

Fig. 2. A–E, overexpression and androgen regulation of TPD52 protein in prostate cancer. Prostate whole tissue lysates were prepared from benign prostate tissue, cancer, and metastatic tumors. Using an affinity-purified antibody specific for TPD52 peptide, immunoblot analysis demonstrated an up-regulation of TPD52 in prostate cancer and metastatic tissue lysates compared with benign prostate tissue samples (A). TPD52 protein expression was evaluated using high-density tissue microarrays. The tissue microarray analysis reveals strong cytoplasmic TPD52 protein expression in neoplastic prostate tissues [i.e., high-grade prostatic intraepithelial neoplasia, localized prostate cancer, and metastatic prostate cancer (B and C). Weak to moderate TPD52 expression was seen in benign prostate tissue (B, 1 and 2; ×200). Strong protein expression was consistently seen in localized prostate cancer samples (B, 3 and 4; ×200) and metastatic prostate cancer (B, 5; ×200). TPD52 expression was confined to the cytoplasm and was not observed in the nucleus (B, 6; ×600). Protein expression was strongest in localized and metastatic prostate cancer. The mean TPD52 protein expression levels are presented in C using error bars with 95% confidence intervals (Benign, benign prostatic tissue; PIA, atrophic prostatic glands also referred to as proliferative inflammatory atrophy; PIN, high-grade prostatic intraepithelial neoplasia; PCa, clinically localized prostate cancer; Mets, hormone-naïve and -refractory metastatic prostate cancer). Sequence analyses showed the presence of androgen-responsive elements upstream of the *TPD52* gene. The hormone-responsive prostate cancer cell line LNCaP was treated with synthetic androgen R1881 for 24, 48, and 72 h. The lysates from the treated and untreated cells were separated on SDS-PAGE, and immunoblotting was carried out for TPD52 protein expression. Up-regulation of PSA served as a positive control for androgen action (D and E).

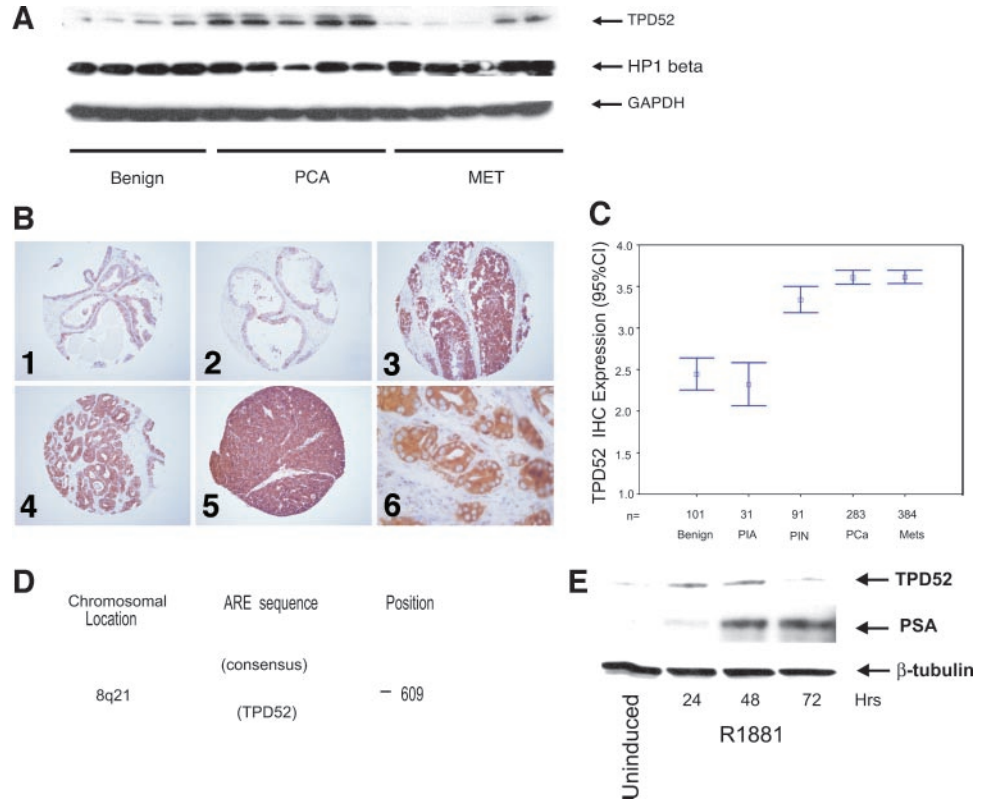


Table 1 *TPD52* protein expression in prostate cancer as determined by immunohistochemistry using TMA<sup>a</sup>

Tissue type	TMA samples	Mean staining intensity <sup>b</sup>	SE	95% CI	
				Low	High
Benign	101	2.45	9.70E-02	2.25	2.64
PIA	31	2.32	0.13	2.07	2.58
PIN	91	3.34	8.00E-02	3.18	3.5
PCA	283	3.61	4.33E-02	3.52	3.69
METS	384	3.61	4.10E-02	3.53	3.69

<sup>a</sup> TMA, tissue microarray; CI, confidence interval; Benign, benign prostate tissue; PIA, proliferative inflammatory atrophy; PIN, high-grade prostatic intraepithelial neoplasia; PCA, clinically localized prostate cancer; METS, hormone-refractory metastatic prostate cancer.

<sup>b</sup> Staining intensity is score from negative (score = 1) to strong (score = 4).

synthetic androgen R1881 over different time points. Up-regulation of PSA served as positive control for androgen action. Stimulation of the LNCaP cells with R1881 demonstrated an expected increase in PSA and a modest increase in TPD52 expression starting at 24 h, and maximum effect was seen at 48 h (Fig. 2E).

**Amplification of *TPD52* as Determined by aCGH and SNP Arrays.** *TPD52* is located in a known area of amplification on chromosome 8q21 (21, 22). This area of chromosome 8q has also been linked to prostate cancer progression (7, 59). Therefore, we set out to determine the extent of chromosome 8q21 amplification in metastatic prostate cancer samples using two independent techniques. Using an aCGH platform containing approximately 2400 BAC clones with an average genome-wide resolution of 1.4 Mb (44, 45), we examined the data for 7 consecutive BACs at 8q21, with one containing *TPD52* (Table 2). Although copy number cannot be accurately determined from this analysis, the BAC containing *TPD52* (clone RP11-214E11) demonstrated a significant copy number increase based on the log<sub>2</sub> ratios for the clinically localized and hormone-refractory metastatic prostate cancers with mean log<sub>2</sub> ratios of 0.24 and 0.30, respectively. Therefore, if one calculates copy gain as a log<sub>2</sub> ratio of ≥0.24, the cases with amplification are presented in Table 2. Approximately 45% (25 of 56) of primary prostate cancers and 63% (5 of 8) metastatic tumors demonstrated a genomic gain at the BAC containing *TPD52*

Table 2 BAC<sup>a</sup> located near *TPD52* locus mapping to 8q21.13

Mapping positions along 8q are based on University of California Southern California August freeze (see “Materials and Methods” for details or refer to <http://genome.ucsc.edu/index.html> for more information regarding each of these clones).

Clone	KB August 2001	Log <sub>2</sub> Ratio (mean)					
		PCa (N)	Est. amp.	S.E.	Mets (N)	Est. amp.	S.E.
RP11-90B7	89791	-0.04 (62)	5/62	0.021	0.15 (8)	3/8	.20
RP11-115D10	90647	0.16 (62)	18/62	0.018	N/A (2)	N/A	N/A
RP11-195P3 <sup>b</sup>	90833	-0.063(54)	4/54	0.019	-0.038(6)	1/6	0.21
RP11-214E11 <sup>b</sup>	91519	0.24 (56)	25/56	0.028	0.30 (8)	5/8	0.21
RP11-93E11 <sup>b</sup>	91964	0.12 (60)	9/60	0.023	0.11 (9)	5/9	0.18
RP11-80C11	92687	0.15 (59)	10/59	0.024	0.34 (9)	5/9	0.12
RP11-257P3	92974	0.18 (57)	19/57	0.024	0.45 (9)	7/9	0.13

<sup>a</sup> BAC, bacterial artificial chromosome; Est. Amp., estimated number of cases amplified using a log<sub>2</sub> ratio of 0.25 at the cutoff point; NA, not available.

<sup>b</sup> Clones closest to *TPD52*.

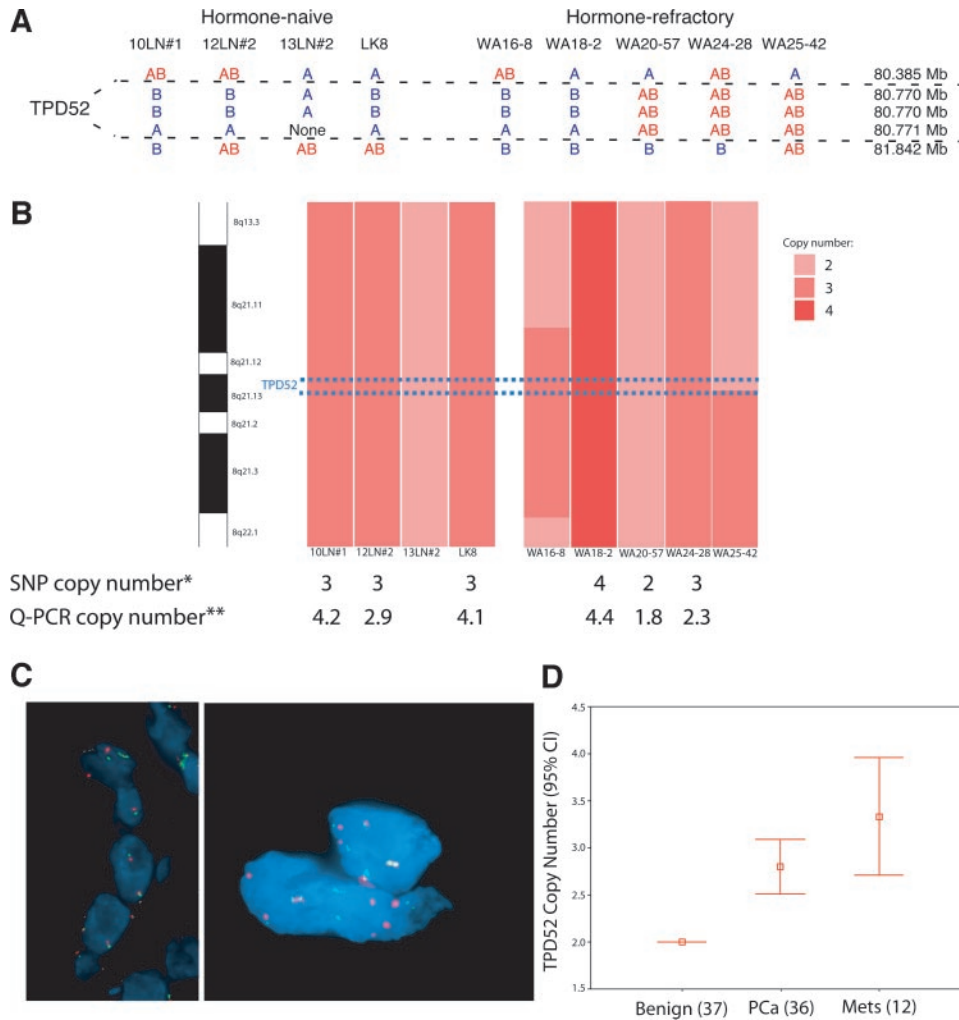


Fig. 3. *A–D*, heterozygosity and amplification on 8q21.13 near TPD52 using single nucleotide polymorphism (SNP) arrays and fluorescent *in situ* hybridization (FISH). *A*, TPD52 is located on chromosome 8q21. By SNP array analysis, we first assessed the level of heterozygosity at TPD52. Alleles identified at SNP loci on chromosome 8 (locations, according to the April 2003 freeze of the human genome, are listed on the *right*) are displayed for hormone-naïve and hormone-refractory prostate cancer metastases. In the germ-line DNA of a given individual, each of the SNP loci probed on the array has an approximately 37% chance of containing both alleles (AB; displayed in *red*) and a 63% chance of being homozygous for one (A or B; displayed in *blue*). A loss of heterozygosity event within a tumor would leave each locus within the affected portion of the genome with only one allele. All of the metastases evaluated, with only one exception (WA18-2), had heterozygous loci either within or immediately adjacent to the region spanned by TPD52 (boundaries are denoted by *dashed lines*). SNP array analysis is regularly unable to identify either allele in 5–10% of the probed loci; this is displayed in *black* as *None*. *B*, a second novel approach was taken combining newly developed SNP chips and novel informatics tools. By comparing the signal intensity at each SNP locus with the intensity of normal controls, amplifications can be identified. Copy numbers along a segment of 8q21 (cytoband reference in *black* on the *left*) are displayed for four hormone-naïve and five hormone-refractory metastatic prostate tumors. The approximate boundaries of TPD52 are denoted by the *dashed blue lines*. Four of five hormone-naïve and three of five hormone-refractory metastases appear to be amplified at TPD52. A fourth hormone-refractory metastasis is amplified adjacent to and possibly overlapping part of the region spanned by TPD52. The region displayed represents data obtained from >60 SNP loci; 3 SNP loci were within the region spanned by TPD52. The results of the SNP copy number estimates are compared with quantitative real-time PCR results *below* the figure. The copy number for the SNPs was determined by Hidden-Markov modeling, and the copy number from quantitative real-time PCR was estimated by averaging results of amplicons overlying exons 2, 4, and 6 of TPD52 (see “Materials and Methods” for details). *C*, FISH analysis was performed using tissue microarrays with a BAC probe specific for a region on the long arm of chromosome 8 containing TPD52 (*red probe*). Amplification was observed in prostate cancer samples (*right panel*) but not in histologically benign prostate tissue from the same patient (*left panel*). The highest mean copy amplification was observed in hormone-refractory prostate cancer (mean copy number, 3.3). The mean copy number for clinically localized prostate cancer was 2.8. Significant copy number increases were seen between benign and clinically localized prostate cancer (mean difference, 0.8; SE, 0.13; *post hoc* Scheffé analysis,  $P < 0.0001$ ) and between localized prostate cancer and hormone-refractory prostate cancer (mean difference, 0.54; SE, 0.13; *post hoc* Scheffé analysis,  $P < 0.001$ ). *D*, the variation in amplification for TPD52 as determined by FISH is presented graphically using *error bars* with 95% confidence intervals. Although this amplification was specific for a BAC containing TPD52, a separate probe using a BAC containing elongin C, located at 8q21, demonstrated amplification (*green probe*). There was no significant difference in amplification between these two BAC probes (data not shown).

(clone RP11-214E11). Best estimates suggest that seven of the clinically localized tumors had a gain of two copies, and eight tumors had a single copy gain. The amplicon width at 8q21 appears to be approximately 1.5 Mb. *Elongin C*, in the region of 8q21.11 and approximately 60 Mb from TPD52, did not demonstrate consistent amplification (data not shown).

A second novel approach was taken using newly developed SNP arrays. We have shown previously (46) that these arrays can robustly detect loss of heterozygosity events in prostate cancers. Alleles identified at SNP loci on chromosome 8 (locations, according to the April 2003 freeze of the human genome, listed on the *right* in Fig. 3A) are

displayed for hormone-naïve and hormone-refractory prostate cancer metastases. In the germ-line DNA of a given individual, each of the SNP loci probed on the array has an approximately 37% chance of containing both alleles (AB, displayed in *red*) and a 63% chance of being homozygous for one (A or B, displayed in *blue*). A loss of heterozygosity event within a tumor would leave each locus within the affected portion of the genome with only one allele. All of the metastases evaluated, with only one exception (WA18-2), had heterozygous loci either within or immediately adjacent to the region spanned by TPD52 (boundaries are denoted by *dashed lines*). SNP array analysis is regularly unable to identify either allele in 5–10% of

Table 3 *TPD52* amplification in prostate cancer progression as determined by FISH<sup>a</sup>

Tissue type (no. of cases) <sup>b</sup>	Mean copy no. (range)	SE	95% CI for mean value	
			Low	High
Benign (38)	2.0(2–2)	0.00	2	2
PCa (37)	2.8(2–6)	0.15	2.5	3.1
Mets (12)	3.3(2–4)	0.05	2.7	4.0

<sup>a</sup> FISH, fluorescence *in situ* hybridization; CI, confidence interval; PCa, clinically localized prostate cancer; Mets, hormone-refractory metastatic prostate cancer.

<sup>b</sup> A minimum of 2 tissue microarray samples/case were evaluated.

the probed loci; this is displayed in *black* as *None*. We were also able to estimate amplification using the SNP arrays by measuring the intensity of expression of each SNP (Fig. 3B). Copy numbers along a segment of 8q21 (cytoband reference in *black* on the *left*) are displayed for four hormone-naïve and four hormone-refractory metastatic prostate tumors. The approximate boundaries of *TPD52* are denoted by the *dashed blue lines*. Three of four hormone-naïve and three of five hormone-refractory metastases are amplified at *TPD52*. A fourth hormone-refractory metastasis is amplified adjacent to (and possibly overlapping part of) the region spanned by *TPD52*. The region displayed represents data obtained from >60 SNP loci; 3 SNP loci were within the region spanned by *TPD52*. Similar to the aCGH data, a copy number increase was seen at *TPD52*. In addition, the SNP analysis was able to define a region of amplification that was seen in the hormone-refractory tumors and, to a lesser degree, in the hormone-naïve metastatic tumors. This region includes *TPD52* and is consistent with previous work that suggests that 8q21 gain is associated with worse clinical outcome (7, 59).

**FISH for *TPD52* Demonstrates an Amplicon at 8q21.** FISH analysis was performed using TMAs with a BAC probe containing *TPD52* (*red probe*). As seen in Fig. 3C, a copy number increase was observed in prostate cancer samples (*right panel*) but not in histologically benign prostate tissue (*left panel*). The highest mean copy increase was observed in hormone-refractory prostate cancer (mean copy number, 3.3). The mean copy number for clinically localized prostate cancer was 2.8. Interestingly, no significant association was seen between Gleason score and copy number. However, the majority of all cases were Gleason score 6 or 7. Table 3 summarizes this data. Significant copy number increases were seen between benign and clinically localized prostate cancer (mean difference, 0.8; SE, 0.13; *post hoc* Scheffé analysis,  $P < 0.0001$ ) and between localized prostate cancer and hormone-refractory prostate cancer (mean difference, 0.54; SE, 0.13; *post hoc* Scheffé analysis,  $P < 0.001$ ). The variation in increased *TPD52* copy number as determined by FISH is presented graphically in Fig. 3D using *error bars* with 95% confidence intervals. Parallel FISH studies using an *Elongin C*-containing BAC (*green*) also located at 8q21 but 60 Mb away confirmed amplification of this region. The FISH analyses did not reveal differences in the incidence of amplification, between the *TPD52* and *Elongin C* probes (data not shown).

***TPD52* Expression in Other Cancers.** Because the expression of *TPD52* was identified in breast and now prostate cancer, we also sought to identify other tumors that may preferentially overexpress *TPD52*. Using ONCOMINE,<sup>14</sup> a new informatics tool developed by our group, we were able to interrogate other expression array data sets that contained information on *TPD52* expression in common human cancers. ONCOMINE contains data from 65 cancer microarray data sets spanning most major types and many subtypes of cancer (60). After the microarray data were normalized and analyzed for differential expression as described previously (60), we searched for cancer

types or subtypes other than breast and prostate cancer in which *TPD52* was differentially expressed. As shown in Fig. 4, *TPD52* is differentially overexpressed in a number of cancer types relative to the normal tissues from which they arose. Confirming previous work, *TPD52* was found to be overexpressed in breast cancer, and interestingly, the ONCOMINE analysis revealed that a study comparing estrogen receptor-positive breast cancer with estrogen receptor-negative breast cancer found *TPD52* to be preferentially overexpressed in the estrogen receptor-positive cases.

## DISCUSSION

Chromosome 8q gain is known to be associated with poor outcome in men with clinically localized prostate cancer (7, 59). The current study identifies a potential oncogene associated with prostate cancer progression. Several pieces of evidence support this observation. First, multiple expression array studies have identified *TPD52* as overexpressed at the transcript level (51). This observation was confirmed using quantitative reverse transcription-PCR. *TPD52* protein overexpression was also observed in prostate cancer using high-density TMAs from a large range of patient samples. By two separate chip-based genomic approaches, amplification of 8q21.13 in the region of *TPD52* was observed, with the greatest increase in copy number occurring in metastatic prostate cancer samples. By contrast, a BAC clone at 8q21.11, located approximately 60 Mb centromeric to *TPD52*, did not demonstrate consistent amplification. The *c-myc* oncogene located at 8q24 has also been found to be variably amplified in prostate cancer (7, 15, 16, 18, 19). One study looking at hormone-refractory prostate tumors demonstrated only 11% amplification for *c-myc*, but this amplification was associated with prostate cancer progression (18). Therefore, it is clear that multiple foci of amplification exist on 8q. The current study also demonstrates that by using high-density SNP-arrays, the resolution should allow for a better appreciation of these amplification events, which could not be identified using FISH probes. The FISH data would suggest that, because both *TPD52* and *Elongin C* probes demonstrated amplification, both genes sit on a large amplicon. However, the SNP and aCGH data presented in this study help us to better appreciate that along this area of 8q, there are several amplification peaks. Both 8q21.11 and 8q21.13 have copy number increases but by SNP analysis and aCGH are shown to represent two discrete areas of amplification on 8q independent of *c-myc*. As the resolution of the SNP chips increases, genomic complexity should be better appreciated.

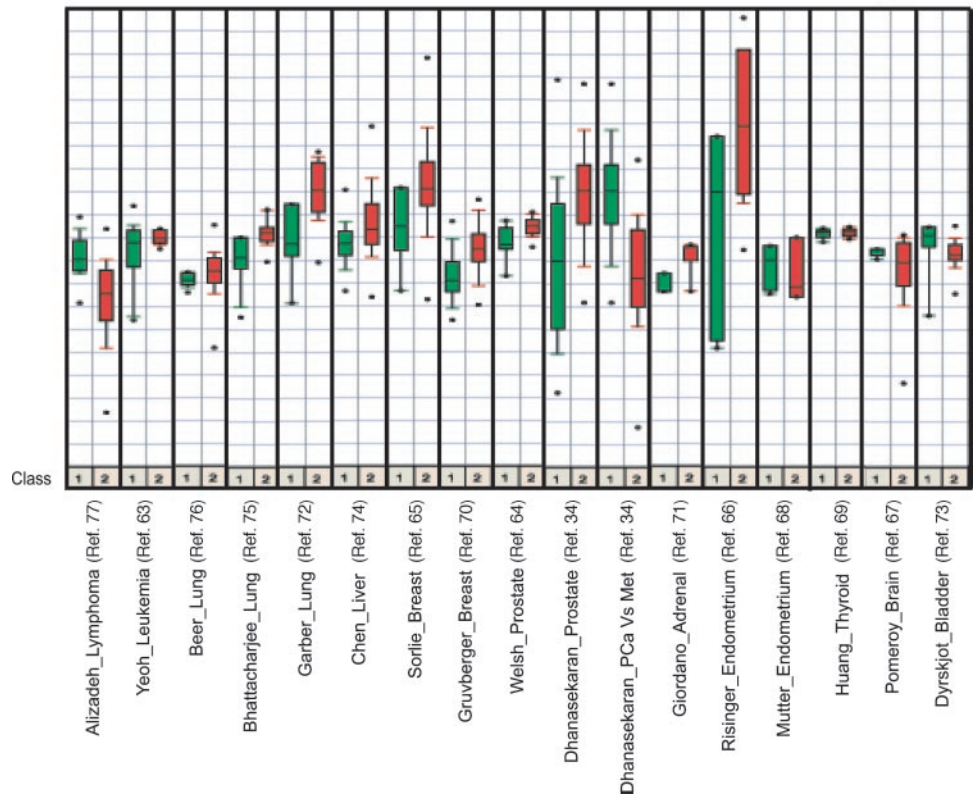
The copy number increase at 8q21.13 cannot be the only explanation for the overexpression of *TPD52* at the protein level. This study found that a significantly larger percentage of localized and metastatic prostate tumors express *TPD52* by immunohistochemistry than demonstrate an increase in copy number at 8q21.13. Therefore, deregulation of *TPD52* cannot be entirely explained by amplification. This study also found that *TPD52* was highly expressed in prostatic intraepithelial neoplasia but not to the same degree of intensity as benign prostate epithelium or proliferative inflammatory atrophy, suggesting that *TPD52* expression may occur early in the development of cancer.

Although further confirmatory work needs to be performed, androgen response elements were identified upstream of the *TPD52* coding region, and cell line experiments provide evidence for the regulation of *TPD52* by androgen incubation. These findings suggest that *TPD52* expression may be regulated in part by androgens, as suggested by work from DePrimo *et al.* (61) and Nelson *et al.* (58). The combination of gene amplification and androgen stimulation likely contributes to the up-regulation of *TPD52*. At this point, it is unclear what role *TPD52* plays in cancer progression. However, the TMA experiments suggest that there was a trend toward PSA failure after radical pros-

<sup>14</sup> www.oncomine.org.

Class 1  
Class 2

Fig. 4. TPD52 expression in different tumors from publicly available cancer microarray studies (34, 63–77). Expression array analysis of multiple cancer microarray data sets was collected and analyzed, and statistical significance was calculated. This was facilitated by our group's ongoing efforts to create a cancer microarray meta-analysis database (see www.ONCOMINE.org). Class 1 represents (unless otherwise indicated) the expression in normal tissues, and class 2 represents expression in cancer. Class 1 in the Alizadeh *et al.* (77) lymphoma study was blood B cells, and class 2 was diffuse large B-cell lymphoma. In the Yeoh *et al.* (63) leukemia study, the comparison was between different acute lymphoblastic leukemia (class 1) and hypodiploid tumors (class 2). The Gruberger *et al.* (70) breast cancer study analyzed estrogen receptor-negative breast cancer (class 1) and estrogen receptor-positive cancer (class 2) cases. The Mutter *et al.* (68) endometrium data represent a comparison between grade 1 endometrioid adenocarcinoma (class 1) and grade 3 endometrioid adenocarcinoma (class 2).



tatectomy with strong TPD52 expression. One limitation with this immunohistochemical analysis is that the vast majority of clinically localized tumors demonstrated moderate to strong TPD52 expression, making a reproducible threshold difficult to achieve using standard techniques. We have begun the process of trying to determine whether the increased amplification seen is closely associated with protein expression. This work will use a highly sensitive fluorescence-based method that we have recently applied to prostate cancer samples using an automated quantitative imaging system called AQUA (62). This should allow us to help distinguish whether there is any difference in TPD52 protein expression between high-grade prostatic intraepithelial neoplasia and localized prostate cancer. Future work will also concentrate on defining the functional role of TPD52 in prostate cancer progression.

This study is the first to combine SNP arrays and aCGH to help characterize a region of amplification. This process allows for confirmation of these genomic observations using two separate technologies. The similar results seen by use of SNPs by one array-based method and BAC probes by another method suggest that SNP array-based technology, which is commercially available, may make this technology available to a broader group of users. The excellent concordance between these two technologies and the FISH results for *TPD52* was very promising.

The use of ONCOMINE, a novel informatics tool, demonstrated an approach to survey multiple expression array studies for a specific gene of interest. Although 8q21 amplification is not universally seen in all cancers, ONCOMINE analysis suggests that both solid and hematopoietic tumors demonstrate overexpression of *TPD52*. It is important in the understanding of cancer biology and biomarker development to determine how widespread perturbations of a single gene are in the neoplastic process. In the current study, *TPD52* was

seen as overexpressed in prostate cancer, as described previously (51, 58), and in other solid and hematopoietic malignancies.

This study also demonstrated the utility of a second novel informatics tool, a module for evaluation of genomic application integrated into dChip (49), used to analyze commercially available SNP arrays. This software was used previously to provide information regarding loss of heterozygosity events in prostate tumors, as reported previously by one of the Lieberfarb *et al.* (46). It has now been upgraded to also allow for evaluation of amplifications and deletions (47). Therefore, using a single chip-based assay, one can in theory perform genome-wide searches for oncogenes and tumor suppressor genes. One can potentially subclassify tumors at resolutions of approximately 300 kb by identifying areas of loss of heterozygosity, homozygous deletions, and areas of amplifications. SNP array technology should greatly enhance our ability to study genomic aberrations associated with carcinogenesis.

In summary, this study demonstrated overexpression of TPD52 in prostate cancer. This overexpression is likely produced by increased gene copy number in a proportion of cases, and it increases with prostate cancer progression. Androgens may positively regulate this expression, as suggested by the presence of androgen response elements located upstream of *TPD52* and regulation of TPD52 protein expression in a prostate cancer cell line study. As demonstrated by a wide survey of expression array data, *TPD52* is overexpressed in tumors other than those of the prostate and breast.

### Addendum

While this paper was in review, another group reported on PrLZ, a family member of TPD52.

Wang R, Xu J, Saramaki O, Visakorpi T, Sutherland WM, Zhou J, Sen B, Lim SD, Mabeesh N, Amin M, Dong JT, Petros JA, Nelson PS, Marshall FF, Zhou HE, and Chung LW. PrIZ, a novel prostate-specific and androgen-responsive gene of the TPD52 family, amplified in chromosome 8q21.1 and overexpressed in human prostate cancer. *Cancer Res* 2004;64:1589–94.

## ACKNOWLEDGMENTS

We thank Lela Schumacher and Srilakshmi Bhagavathula for excellent technical support.

## REFERENCES

- Cher ML, MacGrogan D, Bookstein R, et al. Comparative genomic hybridization, allelic imbalance, and fluorescence in situ hybridization on chromosome 8 in prostate cancer. *Genes Chromosomes Cancer* 1994;11:153–62.
- Macoska JA, Trybus TM, Sakr WA, et al. Fluorescence in situ hybridization analysis of 8p allelic loss and chromosome 8 instability in human prostate cancer. *Cancer Res* 1994;54:3824–30.
- Macoska JA, Trybus TM, Benson PD, et al. Evidence for three tumor suppressor gene loci on chromosome 8p in human prostate cancer. *Cancer Res* 1995;55:5390–5.
- Haggman MJ, Wojno KJ, Pearsall CP, Macoska JA. Allelic loss of 8p sequences in prostatic intraepithelial neoplasia and carcinoma. *Urology* 1997;50:643–7.
- Macoska JA, Trybus TM, Wojno KJ. 8p22 loss concurrent with 8c gain is associated with poor outcome in prostate cancer. *Urology* 2000;55:776–82.
- Joos S, Bergerheim US, Pan Y, et al. Mapping of chromosomal gains and losses in prostate cancer by comparative genomic hybridization. *Genes Chromosomes Cancer* 1995;14:267–76.
- Nupponen NN, Kakkola L, Koivisto P, Visakorpi T. Genetic alterations in hormone-refractory recurrent prostate carcinomas. *Am J Pathol* 1998;153:141–8.
- Saramaki O, Willi N, Bratt O, et al. Amplification of EIF3S3 gene is associated with advanced stage in prostate cancer. *Am J Pathol* 2001;159:2089–94.
- Visakorpi T, Kallioniemi AH, Syvanen AC, et al. Genetic changes in primary and recurrent prostate cancer by comparative genomic hybridization. *Cancer Res* 1995; 55:342–7.
- Nupponen NN, Porkka K, Kakkola L, et al. Amplification and overexpression of p40 subunit of eukaryotic translation initiation factor 3 in breast and prostate cancer. *Am J Pathol* 1999;154:1777–83.
- Nupponen NN, Isola J, Visakorpi T. Mapping the amplification of EIF3S3 in breast and prostate cancer. *Genes Chromosomes Cancer* 2000;28:203–10.
- Porkka K, Saramaki O, Tanner M, Visakorpi T. Amplification and overexpression of elongin C gene discovered in prostate cancer by cDNA microarrays. *Lab Invest* 2002;82:629–37.
- Tan JM, Tock EP, Chow VT. The novel human MOST-1 (C8orf17) gene exhibits tissue specific expression, maps to chromosome 8q24.2, and is overexpressed/amplified in high grade cancers of the breast and prostate. *Mol Pathol* 2003;56:109–15.
- Jackson-Cook C, Zou Y, Turner K, Astbury C, Ware J. A novel tumorigenic human prostate epithelial cell line (M2205): molecular cytogenetic characterization demonstrates C-MYC amplification and jumping translocations. *Cancer Genet Cytogenet* 2003;141:56–64.
- Reiter RE, Sato I, Thomas G, et al. Coamplification of prostate stem cell antigen (PSCA) and MYC in locally advanced prostate cancer. *Genes Chromosomes Cancer* 2000;27:95–103.
- Jenkins RB, Qian J, Lieber MM, Bostwick DG. Detection of c-myc oncogene amplification and chromosomal anomalies in metastatic prostatic carcinoma by fluorescence in situ hybridization. *Cancer Res* 1997;57:524–31.
- Reiter RE, Gu Z, Watabe T, et al. Prostate stem cell antigen: a cell surface marker overexpressed in prostate cancer. *Proc Natl Acad Sci USA* 1998;95:1735–40.
- Bubendorf L, Kononen J, Koivisto P, et al. Survey of gene amplifications during prostate cancer progression by high-throughput fluorescence in situ hybridization on tissue microarrays. *Cancer Res* 1999;59:803–6.
- Mark HF, Samy M, Santoro K, Mark S, Feldman D. Fluorescent in situ hybridization study of c-myc oncogene copy number in prostate cancer. *Exp Mol Pathol* 2000;68: 65–9.
- Byrne JA, Tomasetto C, Garnier JM, et al. A screening method to identify genes commonly overexpressed in carcinomas and the identification of a novel complementary DNA sequence. *Cancer Res* 1995;55:2896–903.
- Pollack JR, Sorlie T, Perou CM, et al. Microarray analysis reveals a major direct role of DNA copy number alteration in the transcriptional program of human breast tumors. *Proc Natl Acad Sci USA* 2002;99:12963–8.
- Balleine RL, Fejzo MS, Sathasivam P, et al. The hD52 (TPD52) gene is a candidate target gene for events resulting in increased 8q21 copy number in human breast carcinoma. *Genes Chromosomes Cancer* 2000;29:48–57.
- Greene F L, American Joint Committee on Cancer, American Cancer Society. AJCC cancer staging manual, 6th ed, New York: Springer-Verlag; 2002. p. xiv.
- Gleason DF. Histologic grade, clinical stage, and patient age in prostate cancer. *Natl Cancer Inst Monogr* 1988;7:15–8.
- Gleason DF. Classification of prostatic carcinomas. *Cancer Chemother Rep* 1966;50: 125–8.
- Rubin MA, Putzi M, Mucci N, et al. Rapid (“warm”) autopsy study for procurement of metastatic prostate cancer. *Clin Cancer Res* 2000;6:1038–45.
- Kleer CG, Cao Q, Varambally S, et al. EZH2 is a marker of aggressive breast cancer and promotes neoplastic transformation of breast epithelial cells. *Proc Natl Acad Sci USA* 2003;100:11606–11.
- Fink L, Seeger W, Emert L, et al. Real-time quantitative RT-PCR after laser-assisted cell picking. *Nat Med* 1998;4:1329–33.
- Westerman BA, Neijenhuis S, Poutsma A, et al. Quantitative reverse transcription-polymerase chain reaction measurement of HASH1 (ASCL1), a marker for small cell lung carcinomas with neuroendocrine features. *Clin Cancer Res* 2002;8:1082–6.
- Qian Z, Fernald AA, Godley LA, Larson RA, Le Beau MM. Expression profiling of CD34+ hematopoietic stem/progenitor cells reveals distinct subtypes of therapy-related acute myeloid leukemia. *Proc Natl Acad Sci USA* 2002;99:14925–30.
- Vandesompele J, De Preter K, Pattyn F, et al. Accurate normalization of real-time quantitative RT-PCR data by geometric averaging of multiple internal control genes. *Genome Biol* 2002;3:RESEARCH0034.
- Prasad S, Thraves P, Dritschilo A, Kuettel M. Expression of cytokeratin-19 as a marker of neoplastic progression of human prostate epithelial cells. *Prostate* 1998; 35:203–11.
- Xue Y, Smedts F, Umbas R, et al. Changes in keratin expression during the development of benign prostatic hyperplasia. *Eur Urol* 1997;32:332–8.
- Dhanasekaran SM, Barrette TR, Ghosh D, et al. Delineation of prognostic biomarkers in prostate cancer. *Nature (Lond)* 2001;412:822–6.
- Zhou M, Chinnaiyan AM, Kleer CG, Lucas PC, Rubin MA. Alpha-methylacyl-CoA racemase: a novel tumor marker over-expressed in several human cancers and their precursor lesions. *Am J Surg Pathol* 2002;26:926–31.
- Mucci NR, Akdas G, Manely S, Rubin MA. Neuroendocrine expression in metastatic prostate cancer: evaluation of high throughput tissue microarrays to detect heterogeneous protein expression. *Hum Pathol* 2000;31:406–14.
- Rubin MA, Mucci NR, Figurski J, et al. E-cadherin expression in prostate cancer: a broad survey using high-density tissue microarray technology. *Hum Pathol* 2001;32: 690–7.
- Varambally S, Dhanasekaran SM, Zhou M, et al. The polycomb group protein EZH2 is involved in progression of prostate cancer. *Nature (Lond)* 2002;419:624–9.
- Xin W, Rhodes DR, Ingold C, Chinnaiyan AM, Rubin MA. Dysregulation of the annexin family protein family is associated with prostate cancer progression. *Am J Pathol* 2003;162:255–61.
- Kononen J, Bubendorf L, Kallioniemi A, et al. Tissue microarrays for high-throughput molecular profiling of tumor specimens. *Nat Med* 1998;4:844–7.
- Perrone EE, Theoharis C, Mucci NR, et al. Tissue microarray assessment of prostate cancer tumor proliferation in African-American and white men. *J Natl Cancer Inst (Bethesda)* 2000;92:937–9.
- Rubin MA, Dunn R, Strawderman M, Pienta KJ. Tissue microarray sampling strategy for prostate cancer biomarker analysis. *Am J Surg Pathol* 2002;26:312–9.
- Paris PL, Albertson DG, Alers JC, et al. High-resolution analysis of paraffin-embedded and formalin-fixed prostate tumors using comparative genomic hybridization to genomic microarrays. *Am J Pathol* 2003;162:763–70.
- Pinkel D, Seagraves R, Sudar D, et al. High resolution analysis of DNA copy number variation using comparative genomic hybridization to microarrays. *Nat Genet* 1998; 20:207–11.
- Snijders AM, Nowak N, Seagraves R, et al. Assembly of microarrays for genome-wide measurement of DNA copy number. *Nat Genet* 2001;29:263–4.
- Lieberfarb ME, Lin M, Lechpammer M, et al. Genome-wide loss of heterozygosity analysis from laser capture microdissected prostate cancer using single nucleotide polymorphic allele (SNP) arrays and a novel bioinformatics platform dChipSNP. *Cancer Res* 2003;63:4781–5.
- Zhao X, Li C, Paez G, et al. Detection of DNA copy number alterations in human cancers using single nucleotide polymorphism arrays. *Cancer Res* 2004, in press.
- Kennedy GC, Matsuzaki H, Dong S, et al. Large-scale genotyping of complex DNA. *Nat Biotechnol* 2003;21:1233–7.
- Lin MF, Wei L, Sellers WR, et al. dChipSNP: significance curve and clustering of SNP-array-based loss-of-heterozygosity data. *Bioinformatics* 2004, in press.
- Wang Y, Wu MC, Sham JS, et al. Prognostic significance of c-myc and AIB1 amplification in hepatocellular carcinoma. A broad survey using high-throughput tissue microarray. *Cancer (Phila)* 2002;95:2346–52.
- Rhodes DR, Barrette TR, Rubin MA, Ghosh D, Chinnaiyan AM. Meta-analysis of microarrays: interstudy validation of gene expression profiles reveals pathway dysregulation in prostate cancer. *Cancer Res* 2002;62:4427–33.
- Luo J, Duggan DJ, Chen Y, et al. Human prostate cancer and benign prostatic hyperplasia: molecular dissection by gene expression profiling. *Cancer Res* 2001;61: 4683–8.
- Luo J, Dunn T, Ewing C, et al. Gene expression signature of benign prostatic hyperplasia revealed by cDNA microarray analysis. *Prostate* 2002;51:189–200.
- Singh D, Febbo PG, Ross K, et al. Gene expression correlates of clinical prostate cancer behavior. *Cancer Cell* 2002;1:203–9.
- Magee JA, Araki T, Patil S, et al. Expression profiling reveals hepsin overexpression in prostate cancer. *Cancer Res* 2001;61:5692–6.
- Stamey TA, Warrington JA, Caldwell MC, et al. Molecular genetic profiling of Gleason grade 4/5 prostate cancers compared to benign prostatic hyperplasia. *J Urol* 2001;166:2171–7.
- Boutros R, Bailey AM, Wilson SH, Byrne JA. Alternative splicing as a mechanism for regulating 14-3-3 binding: interactions between hD53 (TPD52L1) and 14-3-3 proteins. *J Mol Biol* 2003;332:675–87.
- Nelson PS, Clegg N, Arnold H, et al. The program of androgen-responsive genes in neoplastic prostate epithelium. *Proc Natl Acad Sci USA* 2002;99:11890–5.
- van Dekken H, Alers JC, Damen IA, et al. Genetic evaluation of localized prostate cancer in a cohort of forty patients: gain of distal 8q discriminates between progressors and nonprogressors. *Lab Invest* 2003;83:789–96.

60. Rhodes DR, Yu J, Shanker K, et al. ONCOMINE: a cancer microarray database and data-mining platform. *Neoplasia* 2004;6:1–6.
61. DePrimo SE, Diehn M, Nelson JB, Reiter RE, Matese J, Fero M, Tibshirani R, Brown PO, and Brooks JD. Transcriptional programs activated by exposure of human prostate cancer cells to androgen. *Genome Biol* 2002;3:RESEARCH0032.
62. Rubin MA, Zerkowski MP, Camp RL, et al. Quantitative determination of expression of the prostate cancer protein alpha-methylacyl-CoA racemase (AMACR) using AQUA: a novel paradigm for automated and continuous biomarker measurements. *Am J Pathol* 2004;164:831–40.
63. Yeoh EJ, Ross ME, Shurtleff SA, et al. Classification, subtype discovery, and prediction of outcome in pediatric acute lymphoblastic leukemia by gene expression profiling. *Cancer Cell* 2002;1:133–43.
64. Welsh JB, Sapinoso LM, Su AI, et al. Analysis of gene expression identifies candidate markers and pharmacological targets in prostate cancer. *Cancer Res* 2001;61:5974–8.
65. Sorlie T, Perou CM, Tibshirani R, et al. Gene expression patterns of breast carcinomas distinguish tumor subclasses with clinical implications. *Proc Natl Acad Sci USA* 2001;98:10869–74.
66. Risinger JI, Maxwell GL, Chandramouli GV, et al. Microarray analysis reveals distinct gene expression profiles among different histologic types of endometrial cancer. *Cancer Res* 2003;63:6–11.
67. Pomeroy SL, Tamayo P, Gaasenbeek M, et al. Prediction of central nervous system embryonal tumour outcome based on gene expression. *Nature (Lond)* 2002;415:436–42.
68. Mutter GL, Baak JP, Fitzgerald JT, et al. Global expression changes of constitutive and hormonally regulated genes during endometrial neoplastic transformation. *Gynecol Oncol* 2001;83:177–85.
69. Huang Y, Prasad M, Lemon WJ, et al. Gene expression in papillary thyroid carcinoma reveals highly consistent profiles. *Proc Natl Acad Sci USA* 2001;98:15044–9.
70. Gruvberger S, Ringner M, Chen Y, et al. Estrogen receptor status in breast cancer is associated with remarkably distinct gene expression patterns. *Cancer Res* 2001;61:5979–84.
71. Giordano TJ, Thomas DG, Kuick R, et al. Distinct transcriptional profiles of adrenocortical tumors uncovered by DNA microarray analysis. *Am J Pathol* 2003;162:521–31.
72. Garber ME, Troyanskaya OG, Schluens K, et al. Diversity of gene expression in adenocarcinoma of the lung. *Proc Natl Acad Sci USA* 2001;98:13784–9.
73. Dyrskjot L, Thykjaer T, Kruhoffer M, et al. Identifying distinct classes of bladder carcinoma using microarrays. *Nat Genet* 2003;33:90–6.
74. Chen X, Cheung ST, So S, et al. Gene expression patterns in human liver cancers. *Mol Biol Cell* 2002;13:1929–39.
75. Bhattacharjee A, Richards WG, Staunton J, et al. Classification of human lung carcinomas by mRNA expression profiling reveals distinct adenocarcinoma subclasses. *Proc Natl Acad Sci USA* 2001;98:13790–5.
76. Beer DG, Kardia SL, Huang CC, et al. Gene-expression profiles predict survival of patients with lung adenocarcinoma. *Nat Med* 2002;8:816–24.
77. Alizadeh AA, Eisen MB, Davis RE, et al. Distinct types of diffuse large B-cell lymphoma identified by gene expression profiling. *Nature (Lond)* 2000;403:503–11.